Journal of ELECTRONIC MATERIALS, Vol. 42, No. 1, 2013
DOI: 10.1007/s11664-012-2258-4

Low-Cycle Fatigue Behavior of 95.8Sn-3.5Ag-0.7Cu Solder Joints

Y. TANG,[1,2,4] G.Y. LI,[1,5] and X.Q. SHI[3]

1.—School of Electronic and Information Engineering, South China University of Technology, Guangzhou 510641, China. 2.—School of Information, Zhongkai University of Agriculture and Engineering, Guangzhou 510225, China. 3.—Materials and Packaging Technologies Group, Hong Kong Applied Science and Technology Research Institute, Hong Kong Science Park, Hong Kong, Hong Kong. 4.—e-mail: tangyu_mycauc@163.com. 5.—e-mail: phgyli@scut.edu.cn

Low-cycle fatigue (LCF) behavior of 95.8Sn-3.5Ag-0.7Cu solder joints was investigated over a range of test temperatures (25°C, 75°C, and 125°C), frequencies (0.001 Hz, 0.01 Hz, and 0.1 Hz), and strain ranges (0.78%, 1.6%, and 3.1%). Effects of temperature and frequency on the LCF life were studied. Results show that the LCF lifetime decreases with an increase in test temperature or a decrease of test frequency, which is attributed to the longer exposure time to creep and the stress relaxation mechanism during fatigue testing. A modified Coffin–Manson model considering effects of temperature and frequency on the LCF life is proposed. The fatigue exponent and ductility coefficient were found to be influenced by both the temperature and frequency. By fitting the experimental data, the mathematical relations between the fatigue exponent and temperature, and ductility coefficient and temperature, were analyzed. Scanning electron microscopy (SEM) of the cross-sections and fracture surfaces of failed specimens at different temperature and frequency was applied to verify the failure mechanisms.

Key words: Low-cycle fatigue, temperature effect, frequency effect, Coffin–Manson model, lead-free solder

INTRODUCTION

Portable digital electronic products such as digital cameras, personal digital assistants (PDAs), and cellular phones are growth areas for the electronics manufacturing industry. Product and packaging design trends continue to push for smaller form factor and increased functionalities.[1–3] Solder joints in portable digital electronic devices are continuously subjected to temperature and frequency variations and thermal strain that results from differences in thermal expansion coefficient.[4,5] Since the solder is softer than other components, most of the cyclic stress and strain take place in the solder. Therefore, fatigue failure, especially thermally induced, low-cycle fatigue (LCF) failure, is likely to occur in the solder.[6]

(Received January 13, 2012; accepted August 28, 2012; published online October 3, 2012)

The Sn-Ag-Cu (SAC) solder alloy system is widely used in the electronics industry because of its advantageous mechanical properties and solderability.[1] Therefore, understanding the LCF behavior of the deformation and fracture of SAC solder alloy is important for developing reliable portable digital electronic packages. Kanchanomai and Mutoh[7,8] studied the effect of temperature on the isothermal LCF behavior of 96.5Sn-3.5Ag at a constant frequency of 0.1 Hz and found that the LCF behavior under different temperatures (20°C, 85°C, and 120°C) follows the Coffin–Manson equation. Kanchanomai and Miyashita[9,10] investigated the effect of frequency on isothermal LCF behavior and mechanisms of crack initiation and propagation in 96.5Sn-3.5Ag at a constant temperature of 20°C, and proposed a frequency-modified Coffin–Manson model. Kariya et al.[11] found that the LCF life of Sn-3.5Ag-Bi determined by true fracture ductility in a total axial strain-controlled test could be

represented by the ductility-modified Coffin–Manson relationship. Pang and Xiong[12,13] reported LCF models for 95.5Sn-3.8Ag-0.7Cu and 99.3Sn-0.7Cu solder for two test conditions of 25°C at 1 Hz and 125°C at 0.001 Hz, and the Morrow model was used to describe the LCF behavior of the solder alloys. Kanda et al.[14,15] studied the effect of waveform symmetry on the LCF of the Sn-3.0Ag-0.5Cu solder alloy, and pointed out that under asymmetrical triangular waveforms recrystallization occurs during the fatigue test. Liang[16] reported that grain boundaries of tin-rich phases are weak spots for cracking in LCF tests of 95Sn-5Ag. Although the effects of temperature and frequency on LCF behavior in lead-free solder and the temperature dependence of the fatigue exponent and ductility coefficient were studied, the mathematical relations between the fatigue exponent and temperature, and ductility coefficient and temperature, were not reported. In order to better understand the effects of temperature and frequency on the LCF lifetime and failure mechanisms, LCF testing and analysis of 95.8Sn-3.5Ag-0.7Cu solder joints were carried out for a range of test temperatures and frequencies. The effects of test temperature and frequency on the LCF behavior of 95.8Sn-3.5Ag-0.7Cu solder joints are discussed in detail. SEM observation of the cross-sections and fracture surfaces of failed specimens at different temperatures and frequencies was applied to verify the failure mechanisms. A modified Coffin–Manson model is proposed and used for describing the fatigue behavior.

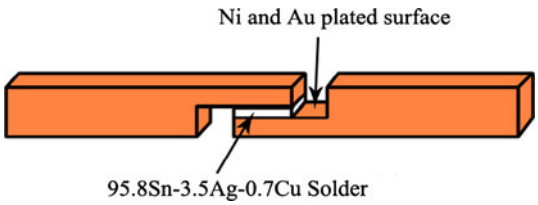

Fig. 1. Schematic of fabrication of shear-lap solder joint specimen.

EXPERIMENTAL PROCEDURES

The lead-free solder alloy used in this study is Sn-3.5 wt.%Ag-0.7 wt.%Cu. For LCF testing, a shear-lap solder joint sample was designed as shown in Fig. 1. The Cu substrates were first ground and polished with 0.25-μm diamond paste until a mirror surface was obtained. The prepared substrates were dipped into 50% (by volume) nitric acid to remove any oxide layer which may be present, and then electroless-plated with a thin layer of Ni (thickness about 3 μm), following by a thin layer of Au (thickness about 0.2 μm). Solder paste of 95.8Sn-3.5Ag-0.7Cu with dimensions of 1.0 mm × 3.2 mm × 0.1 mm was then applied between the two Cu plates. As the amount of solder paste used would affect the fatigue life of the solder joints, care was taken to ensure a uniform layer of solder on each of the Cu substrates. The shear-lap solder joint samples were then passed through a forced convection reflow oven at a peak temperature of 244°C. A typical temperature profile during the reflow soldering process is shown in Fig. 2. The total reflow time is 5.5 min, and the time above the melting temperature of 217°C (eutectic point of Sn-3.5Ag-0.7Cu) is 64 s. After reflow soldering, the sample was mounted onto a stainless-steel grip using an epoxy adhesive for testing.

The fatigue tests were carried out by a micro-force fatigue testing system, with the capacity to produce very low frequencies in a wide range of 0.0001 Hz to 1 Hz. The tests were run under symmetrical

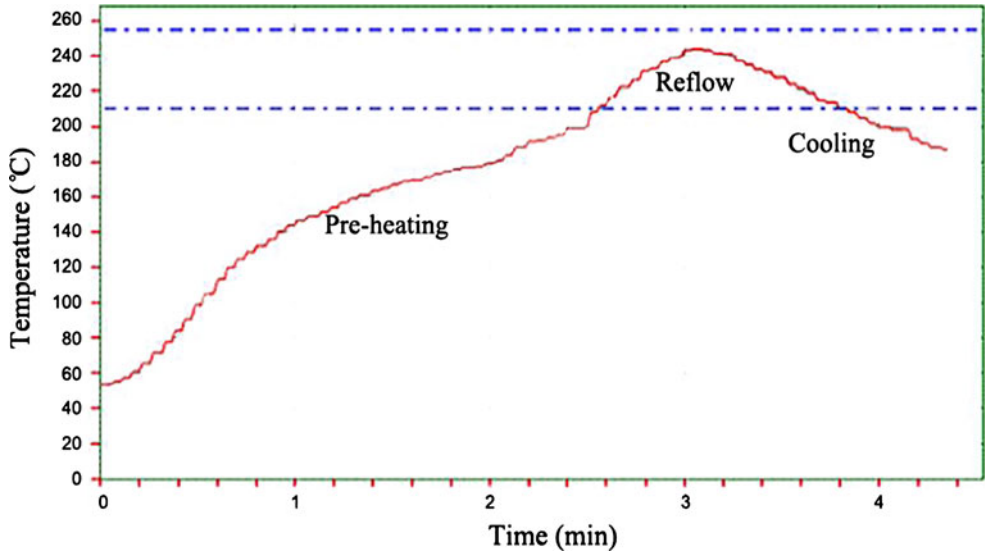

Fig. 2. Typical reflow temperature profile.

uniaxial tension–compression loading with total strain control, which was carried out by using a servohydraulic fatigue machine under 55% relative humidity. For all fatigue tests, the triangular waveform was employed. The testing was conducted at three different total displacement amplitudes of 0.1 mm, 0.05 mm, and 0.025 mm. The three total strain ranges, calculated from the displacement amplitude divided by the gage length (about 3.2 mm), are 3.1%, 1.6%, and 0.78%, respectively. For each of the strain ranges, three different temperatures (25°C, 75°C, and 125°C) and three different frequencies (0.001 Hz, 0.01 Hz, and 0.1 Hz) were selected to conduct experiments. The number of cycles to failure for each of the shear-lap specimens was recorded as the fatigue life. The fatigue failure criterion was a 50% reduction of maximum tensile load, as recommended by the ASTM.[17]

For metallographic observations, shear-lap solder joint samples were first mounted in Klarmount and cross-sectioned perpendicular to the shear-lap solder joints. They were then successively ground down to 1200 grit with silicon carbide paper. Polishing was performed using 5-μm aluminum oxide suspension followed by 0.25-μm diamond paste. The shear-lap solder joint specimens were then etched in a dilute solution of 2% concentrated hydrochloric acid, 6% concentrated nitric acid, and 92% distilled water for about 30 s. SEM was then used to observe the cross-sectional microstructure of the solder joints.

RESULTS AND DISCUSSION

Micrographs of Fracture Surface of Test Samples

Figure 3 shows a typical SEM micrograph of the cross-section of an as-soldered specimen to compare the microstructure of the test samples. The gray areas are the primary β-Sn dendrites, and the light areas are the eutectic phases. The eutectic structure is composed of fine particles of Ag_3Sn and Cu_6Sn_5 intermetallic compounds (IMCs) distributed over the pure Sn matrix.[18]

SEM micrographs of the cross-section and fracture surface of failed specimens tested at frequency of 0.1 Hz and total strain range of 0.78% for the test temperatures of 25°C, 75°C, and 125°C are shown in Fig. 4, respectively. Results show that, with elevating temperature, both the size and number of voids increase, as shown in Fig. 4a–c. Due to the existence of large voids in the interface, the connection areas of solder joints are reduced, and stress concentration occurs in the solder joints. On the other hand, the large voids are the critical trigger points for crack generation as well.[18,19] As a result, the LCF life of solder joints decreases with increase in large voids. With an increase in temperature, the number of cracks on the surface of cross-sections and fracture surfaces of failed specimens

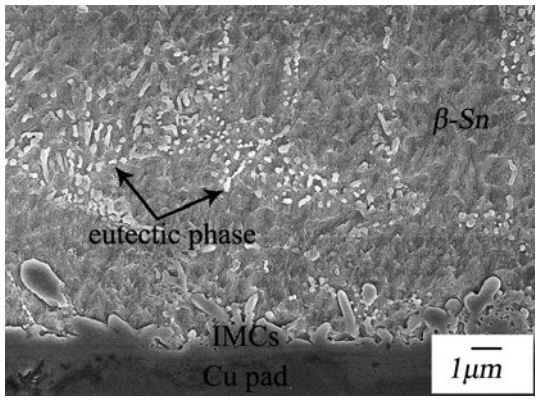

Fig. 3. SEM micrograph of the cross-section of an as-soldered specimen.

increases, as shown in Fig. 4c, f. After elevating the temperature, some of the surface cracks eventually link up to form larger cracks, as shown in Fig. 4f. The propagation of the large crack, indicated by arrows, is intergranular along Sn-dendrite boundaries and transgranular through Ag_3Sn phases, as shown in Fig. 4c. However, no clear evidence of recrystallization enhancing fatigue voiding/cracking was found in our tested samples, similar to the observations by Korhonen et al.[20]

SEM micrographs of the cross-section and fracture surface of failed specimens tested at a temperature of 25°C and strain range of 0.78% for the test frequencies of 0.001 Hz, 0.01 Hz, and 0.1 Hz are shown in Fig. 5. At low frequency, the interfaces between the Sn-dendrites and Sn-Ag eutectic phases become weaker than the matrix and boundary sliding could occur,[19,21] as shown in Fig. 5d. This sliding can cause intergranular fracture during fatigue and shorten fatigue life. This observation is consistent with Kanchanomai et al.,[7,8] who reported that multiple surface cracks predominantly initiate in an intergranular manner along the boundary steps of Sn-dendrite in low-frequency tests. However, boundary sliding is reduced when fine particles are present in the grain boundary. For 95.8Sn-3.5Ag-0.7Cu solder, Sn-Ag eutectic phases are arrested along the boundary of Sn-dendrites. With an increase in frequency, more fine particles are observed, indicated by arrows, as shown in Fig. 5f. The energy-dispersive x-ray spectroscopy (EDX) result shown in Fig. 6 illustrates that the fine particles are Ag_3Sn phase. It should be noted that the fine and uniform dispersion of Ag_3Sn particles could enhance the strength of the alloy by providing more efficient obstacles for dislocation motion. This phenomenon indicates that the LCF life of 95.8Sn-3.5Ag-0.7Cu solder joints increases with increase in frequency. Similar boundary steps and results were systematically observed by Kim and Laird,[22] who studied the crack nucleation phenomena in the LCF of copper.

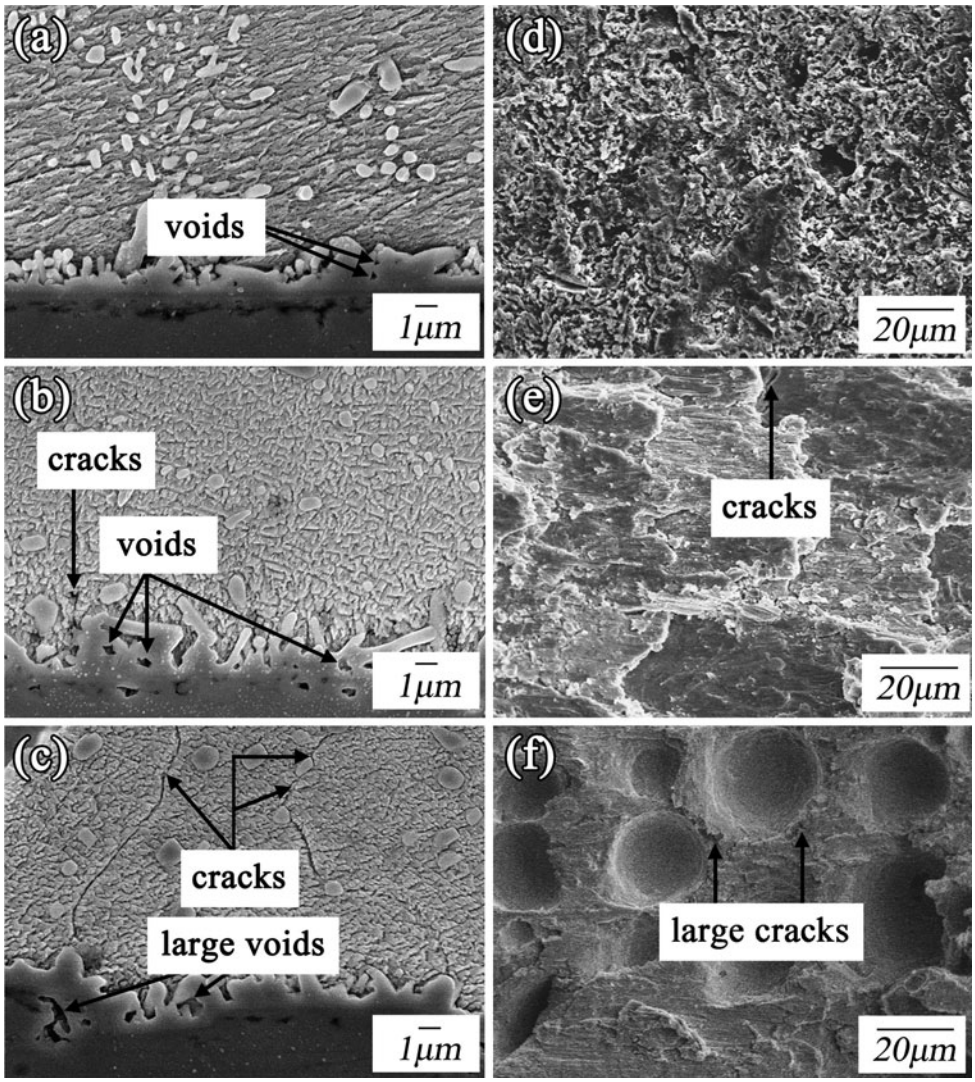

Fig. 4. SEM micrographs of the cross-section and fracture surface of failed specimens tested at 0.1 Hz and total strain range of 0.78% with different test temperatures: (a, d) 25°C; (b, e) 75°C; (c, f) 125°C.

As discussed above, the size and number of voids increase with decreasing frequency. However, when the test frequency was set at 0.1 Hz, voids were not found at the interface, as shown in Fig. 5c. With decreasing frequency, it can be found that both the size and number of cracks increase, indicated by arrows, as shown in Fig. 5d. Small dimples shown in Fig. 5f can be seen on the fracture surface when the test frequency is set to be 0.1 Hz. As the frequency decreases to 0.01 Hz and 0.001 Hz, the fracture surface exhibits sheared dimples, as shown in Fig. 5e, d. These phenomena illustrate that testing frequency could affect the LCF life of the solder joints, which is in agreement with the results observed by Pand and Xiong et al.,[12] who reported that the LCF life of 99.3Sn-0.7Cu solder joints depends on lower test frequency. Our results also reveal that the LCF life depends weakly on the frequency when the test frequency is set to be above 0.01 Hz.

Effects of Test Temperature, Strain Range, and Frequency on Fatigue Life

The variation of fatigue life of shear-lap solder joints under different test temperature, frequency, and strain range is presented in Table I. From Table I, it can be seen that the fatigue life of shear-lap solder joints is affected by test temperature, frequency, and strain range. Fatigue life decreases with increase in temperature under different test frequency and strain range. The log–log plot relationship between fatigue life of shear-lap solder joints and temperature at 0.1 Hz for the total strain ranges of 0.78%, 1.6%, and 3.1% is shown in Fig. 7. The fatigue life of shear-lap solder joints decreases

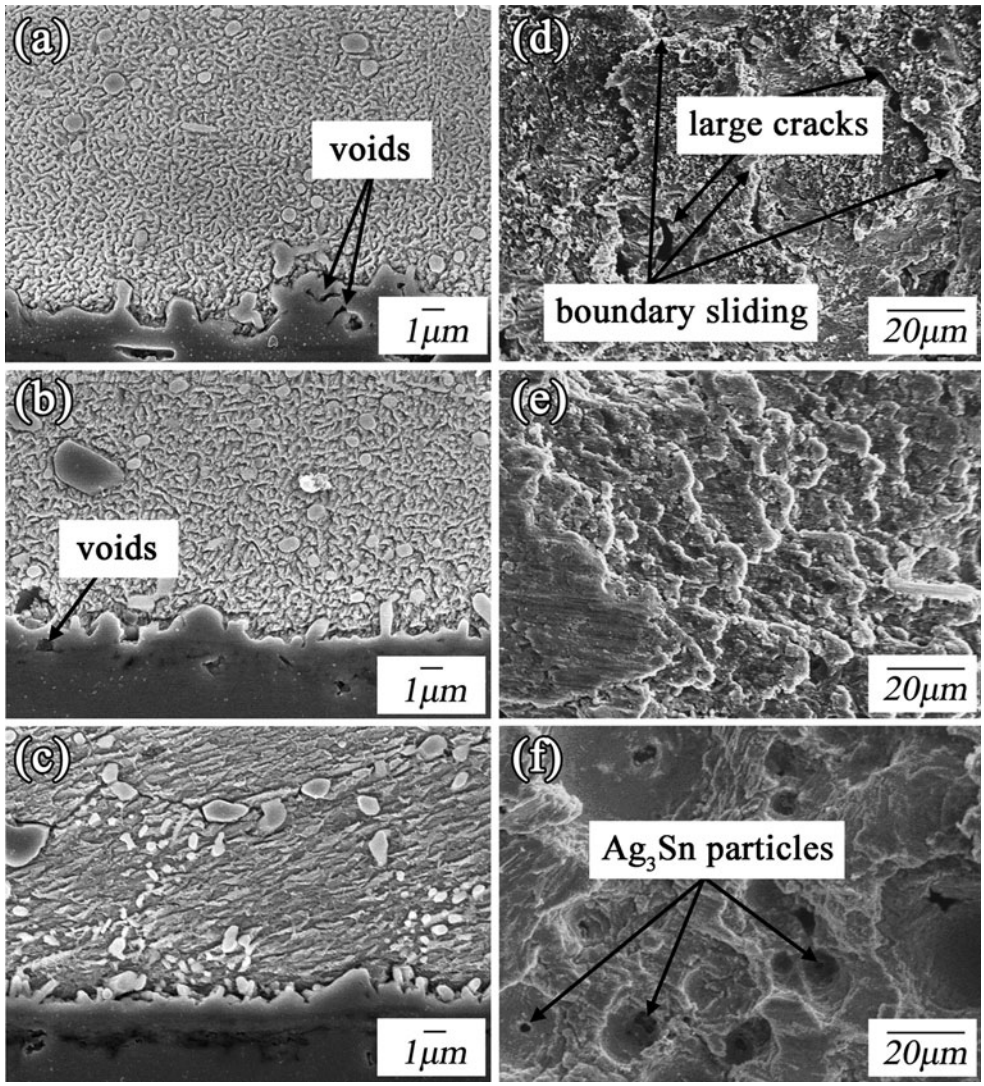

Fig. 5. SEM micrographs of the cross-section and fracture surface of failed specimens tested at 25°C and total strain range of 0.78% with different test frequencies: (a, d) 0.001 Hz; (b, e) 0.01 Hz; (c, f) 0.1 Hz.

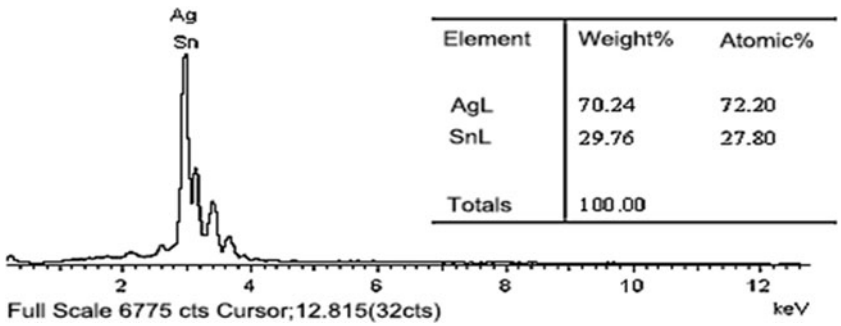

Fig. 6. EDX analysis of fine particles indicated in Fig. 5f.

linearly with increase in test temperature over the temperature range from 25°C to 125°C due to the increment of the number of cracks on the surface of the specimen, which is in agreement with the results observed by Kanchanomai and Mutoh et al.[7,8] This is because, at higher temperature, the creep effect is more significant and the contribution of creep is expected to increase with increase in temperature, which could result in decrease of the fatigue life.[23–25]

Table I. Fatigue life (cycles) of shear-lap solder joints under different test temperature, strain range, and frequency

Test Frequency (Hz)	Test Temperature (°C)	Fatigue Life (cycles) $\Delta\varepsilon_T$ = 0.78%	$\Delta\varepsilon_T$ = 1.6%	$\Delta\varepsilon_T$ = 3.1%
0.001	25	368.5	20.5	10.1
	75	219.4	13.1	4.2
	125	67.2	3.6	0.2
0.01	25	1266.5	113	85
	75	738.6	85.4	12.9
	125	316.1	13.7	1.8
0.1	25	1377.5	143.1	98.5
	75	1036.1	105.1	20.2
	125	429.5	26.8	4.7

From Table I, it can be found that fatigue life also decreases with increase in strain range under any given test temperature and frequency. Generally, the relationship between the plastic strain range and the number of cycles to failure follows the Coffin–Manson equation[7–13]

$$\Delta\varepsilon_p N_f^n = B, \quad (1)$$

where $\Delta\varepsilon_p$ represents the plastic strain range, N_f stands for the fatigue life of shear-lap solder joints, n is the fatigue exponent, and B is the fatigue ductility coefficient.

The Coffin–Manson equation assumes that fatigue life is strictly due to plastic deformation and the elastic strain range has a negligible effect on the LCF life. To meet the requirement of the Coffin–Manson equation, the plastic strain range $\Delta\varepsilon_p$ is calculated from Maxwell's viscoelastic model[26] in this study. Figure 8 shows a log–log plot of plastic strain range versus fatigue life of shear-lap solder joints at the frequency of 0.1 Hz for various temperatures. From Fig. 8, it can be seen that the plastic strain range has a linear relationship with the fatigue life. The fatigue life of the shear-lap solder joints decreases with an increase in plastic strain range at any given temperature. The reason might be that the fatigue life of the specimens is correlated with the true fracture ductility, which increases with an increase in strain range. This will lead to the number of cycles to failure decreasing with an increase in strain range.

The values of the fatigue exponent n and ductility coefficient B can be determined by taking the slope and the intercept on the axis of plastic strain range respectively, as shown in Fig. 9. The fatigue exponent n is found to decrease from 0.45 to 0.30 with the increment of test temperature from 25°C to 125°C. The ductility coefficient B decreases from 0.19 to 0.046 with increase in test temperature. The constants n and B exhibit good linearly relations with the test temperature, respectively.

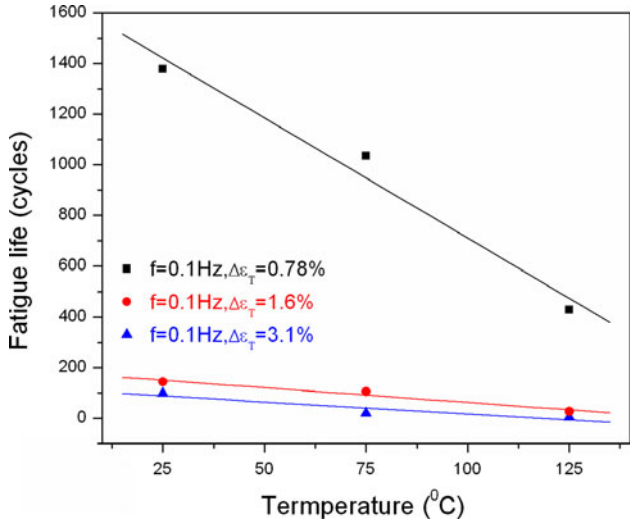

Fig. 7. Relationship between fatigue life of shear-lap solder joints and temperature at 0.1 Hz for three different total strain ranges.

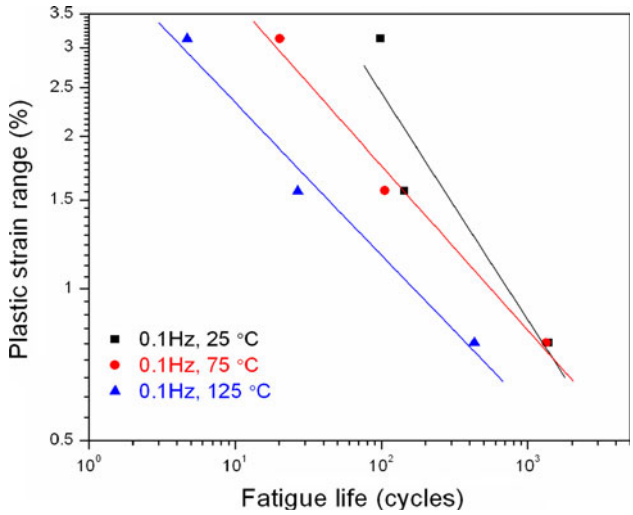

Fig. 8. Plastic strain versus fatigue life of shear-lap solder joints at 0.1 Hz for three different temperatures.

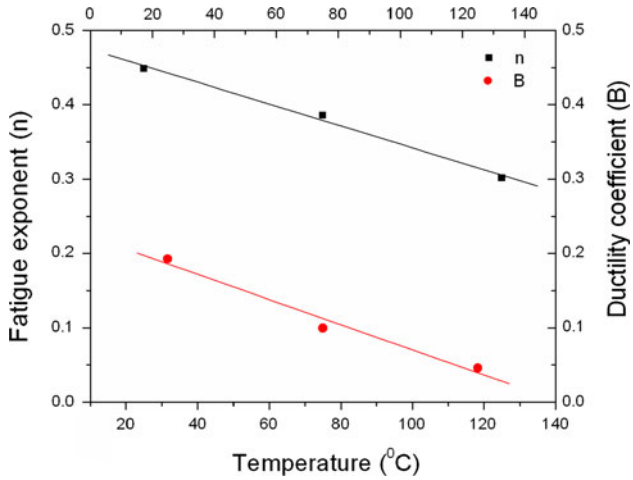

Fig. 9. Coffin–Manson model constants (n and B) as a function of temperature at 0.1 Hz.

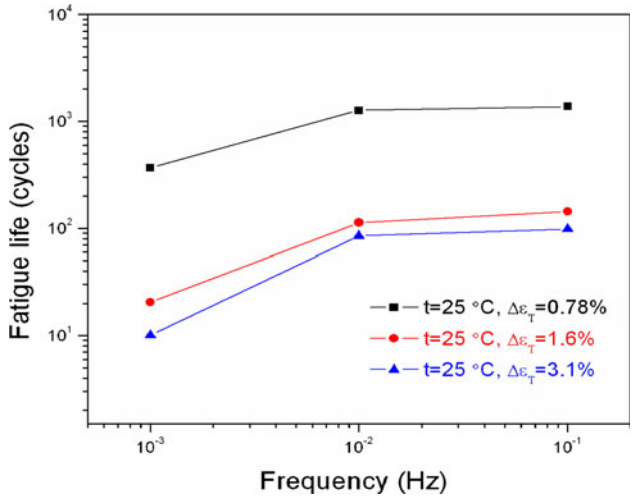

Fig. 10. Fatigue life of shear-lap solder joints versus frequency at 25°C for three total strain ranges.

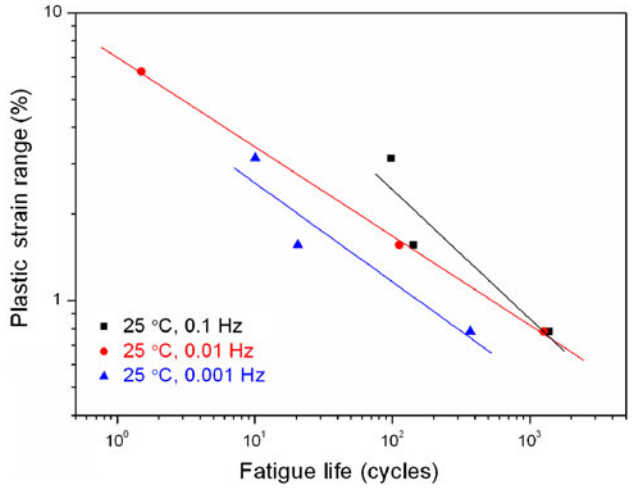

Fig. 11. Plastic strain versus fatigue life of shear-lap solder joints at 25°C for three different frequencies.

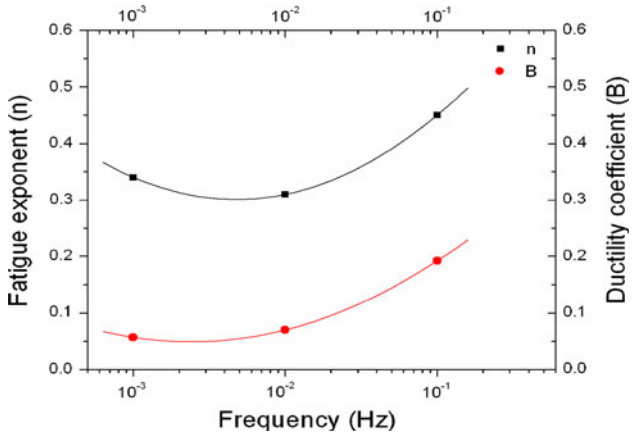

Fig. 12. Coffin–Manson model constants (*n* and *B*) as a function of frequency at 25°C.

It can be found from Table I that the fatigue life decreases with decreasing frequency under any given test temperature and strain range. The variation of fatigue life of shear-lap solder joints with frequency (0.001 Hz, 0.01 Hz, and 0.1 Hz) at 25°C is shown in Fig. 10. It can be seen that the fatigue life of shear-lap solder joints decreases with decreasing frequency, which is attributed to the longer exposure time to creep and the stress relaxation mechanism during fatigue testing. As the frequency increases, the time for completing one cycle decreases. The fatigue life of shear-lap solder joints increases quickly when the frequency is below 0.01 Hz. However, it is weakly dependent on frequency when the frequency is above 0.01 Hz. This result is consistent with the results of Pand and Xiong et al.[12,13]

A log–log plot of plastic strain range versus fatigue life of shear-lap solder joints at 25°C for the frequencies of 0.001 Hz, 0.01 Hz, and 0.1 Hz is shown in Fig. 11. It can be seen that the fatigue exponent n and ductility coefficient B can be determined as a function of frequency at 25°C, as shown in Fig. 12. Results show that the fatigue exponent n ranges from 0.34 to 0.45 as the frequency changes from 0.001 Hz to 0.1 Hz. The ductility coefficient B ranges from 0.057 to 0.192 as the frequency changes from 0.001 Hz to 0.1 Hz. Both n and B increase with the increment of frequency. However, the values of the ductility coefficient B show only a slight change with increase in frequency when the frequency is below 0.01 Hz, which is due to the brittle fracture at the shear-lap solder joint and IMC interface.

A Prediction Model for Fatigue Life

The fatigue exponent n and ductility coefficient B for the Coffin–Manson model are given in Table II. For the test frequency of 0.1 Hz, the fatigue exponent n ranges from 0.45 at 25°C to 0.30 at 125°C. In contrast, the ductility coefficient B ranges from 0.192 at 25°C to 0.047 at 125°C. It can be found that the fatigue exponents for different frequencies only change slightly, while the ductility coefficients increase with increase in frequency and lowering temperature, which means that the Coffin–Manson constant B depends on both the frequency and temperature.

Table II. Coffin–Manson model constants (*n* and *B*) at different temperature and frequency

	n			***B***		
	0.001 Hz	**0.01 Hz**	**0.1 Hz**	**0.001 Hz**	**0.01 Hz**	**0.1 Hz**
25°C	0.34	0.31	0.45	0.057	0.07	0.192
75°C	0.38	0.39	0.35	0.053	0.064	0.095
125°C	0.37	0.31	0.3	0.037	0.044	0.047

Kanchanomai et al.[7–10,27] and Pang et al.[12,13,23,24] reported that the influence of frequency on fatigue life can be described in terms of a frequency-modified Coffin–Manson relationship:

$$(N_f v^{k-1})^n \Delta\varepsilon_p = B, \tag{2}$$

where v and k are the frequency and frequency exponent, respectively, evaluated from the fatigue life–frequency relationship.

If the plastic strain range is kept constant, the fatigue life has a linear relationship with frequency in the logarithmic coordinate. The value of $(1-k)$ can be obtained from the slope of the plots. From Fig. 10, it can be seen that the fatigue life of shear-lap solder joints depends slightly on frequency as the frequency ranges from 0.01 Hz to 0.1 Hz. However, the fatigue life of shear-lap solder joints depends strongly on frequency as the frequency ranges from 0.001 Hz to 0.01 Hz. Therefore, the value of the frequency exponent was calculated in two frequency ranges in this work, corresponding to the value calculated by Pand and Xiong et al.[12,13] Based on our experimental data, Eq. 2 can be modified as:

$$\begin{cases} (N_f v^{k_1-1})^n \Delta\varepsilon_p = B & (0.1\ \text{Hz} \geq v \geq 0.01\ \text{Hz}) \\ \left[N_f \left(\frac{v}{0.01}\right)^{(k_2-1)} (0.01)^{(k_1-1)}\right]^n \Delta\varepsilon_p = B & (0.01\ \text{Hz} > v \geq 0.001\ \text{Hz}) \end{cases} \tag{3}$$

where k_1, k_2, n, and B are dependent on temperature.

Figure 13 shows plots of the frequency exponents (k_1 and k_2) versus temperature at any given plastic stain range. It can be seen that the frequency exponents k_1 and k_2 are 0.93 and 0.27 at 25°C, respectively. When the temperature increases to 75°C, the frequency exponents k_1 and k_2 are 0.52 and 0.25. At 125°C, the frequency exponents (k_1 and k_2) are 0.90 and 0.54. By fitting the data, the relationships between the frequency exponents and temperature can be represented as:

$$k_1 = 19.8 - 0.11T + 1.58 \times 10^{-4} T^2 \tag{4}$$

$$k_2 = 6.82 - 0.04T + 6.2 \times 10^{-5} T^2 \tag{5}$$

Based on Eqs. 4 and 5, the frequency exponents k_1 and k_2 were calculated to be 0.90 and 0.48, respectively, at a test temperature of about 398 K. This result is consistent with the results reported by Pang et al.,[12] where the frequency exponent k_1 was determined to be 0.91 at 398 K as the frequency ranged from 0.01 Hz to 0.1 Hz.

Figure 14 shows plots of the constants n and B versus temperature in the frequency-modified Coffin–Manson model. In order to plot the constants n and B as a function of temperature for the frequency-modified Coffin–Manson model, the values of n and B are averaged at different frequencies. By fitting the data, the constants n and B can be represented as:

$$n = -9.27 + 0.06T - 8.36 \times 10^{-5} T^2 \tag{6}$$

$$B = -20.84 + 0.12T - 1.79 \times 10^{-4} T^2 \tag{7}$$

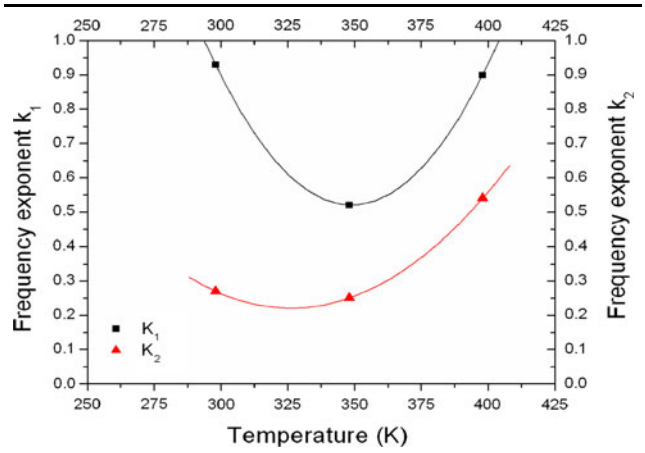

Fig. 13. Frequency exponents versus temperature.

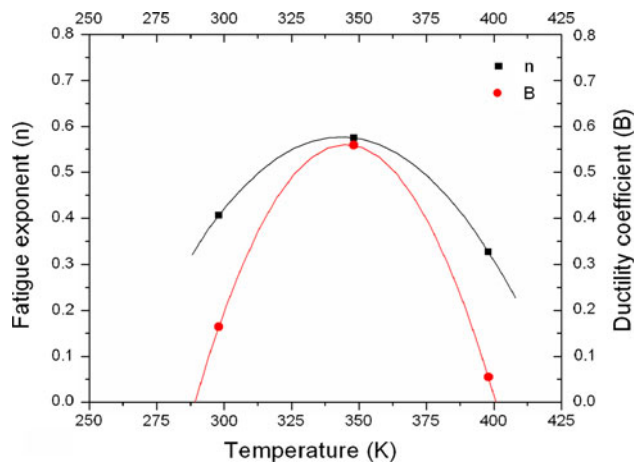

Fig. 14. Relationship between the constants n and B and temperature.

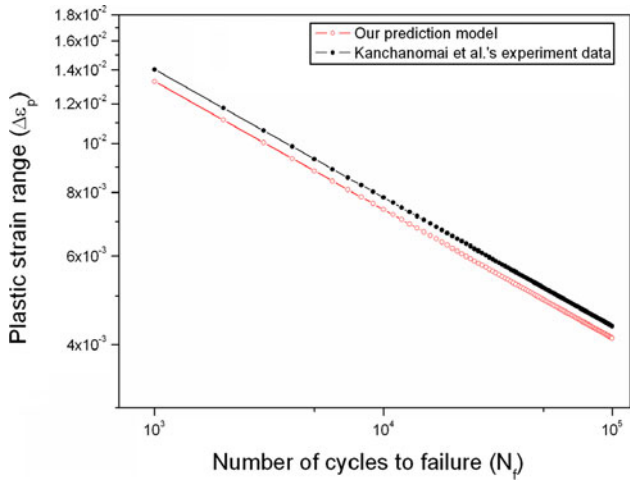

Fig. 15. Verification of the reasonability of our prediction model using Kanchanomai et al.'s experiment data.

Putting the LCF test data for 96.5Sn-3.0Ag-0.5Cu at 0.1 Hz and room temperature of 20°C[9,10] into our model, the relationship between the plastic strain range and the number of cycles to failure can be drawn as shown in Fig. 15. Results show that the fatigue life in our prediction model is slightly lower compared with Kanchanomai et al.'s experimental data.[9] This may be due to the different failure criterion used by Kanchanomai (25% load drop of the stress amplitude).

CONCLUSIONS

The LCF data of 95.8Sn-3.5Ag-0.7Cu shear-lap solder joints at three temperatures (25°C, 75°C, and 125°C) and three frequencies (0.001 Hz, 0.01 Hz, and 0.1 Hz) have been investigated using three values of total strain range (0.78%, 1.6%, and 3.1%). The main conclusions obtained are as follows:

1. The LCF life of 95.8Sn-3.5Ag-0.7Cu shear-lap solder joints is dependent on the test temperature and frequency. Fatigue life decreases with increase in test temperature, but decreases with decrease of test frequency, which is attributed to the longer exposure time to creep and the stress relaxation mechanism during fatigue testing.
2. The LCF behavior for different temperatures of 25°C, 75°C, and 125°C follows the Coffin–Manson equation. The fatigue exponent is found to decrease from 0.45 to 0.30 with increment of test temperature from 25°C to 125°C, while the ductility coefficient decreases from 0.19 to 0.046 with increase in test temperature.
3. The LCF behavior for the frequencies of 0.001 Hz, 0.01 Hz, and 0.1 Hz follows the frequency-modified Coffin–Manson model. At a test temperature of 25°C, the fatigue exponent ranges from 0.34 at 0.001 Hz to 0.45 at 0.1 Hz, and the ductility coefficient ranges from 0.057 at 0.001 Hz to 0.192 at 0.1 Hz. The fatigue exponent and ductility coefficient increase with increment of frequency.
4. A modified Coffin–Manson model considering the effect of temperature and frequency on the LCF life is proposed. By fitting the experimental data, the mathematical relations between the fatigue exponent and temperature, and ductility coefficient and temperature, are given.

REFERENCES

1. G.Y. Li, X.D. Bi, Q. Chen, and X.Q. Shi, *J. Electron. Mater.* 40, 165 (2011).
2. G. Zeng, S. Xue, L. Zhang, L. Gao, W. Dai, and J. Luo, *J. Mater. Sci. Mater. Electron.* 21, 421 (2010).
3. Y.D. Han, H.Y. Jing, S.M.L. Nai, L.Y. Xu, and C.M. Tan, *J. Electron. Mater.* 39, 223 (2010).
4. G.Y. Li, B.L. Chen, and J.N. Tey, *IEEE Trans. Adv. Packag.* 27, 77 (2004).
5. M.R. Harrison, J.H. Vincent, and A.A.H. Steen, *Solder. Surf. Mt. Technol.* 13, 21 (2001).
6. T. Laurila, T. Mattila, V. Vuorinen, J. Karppinen, L. Li, M. Sippola, and J.K. Kivilahti, *Microelectron. Reliab.* 47, 1135 (2007).
7. C. Kanchanomai and Y. Mutoh, *Mater. Sci. Eng. A* 381, 113 (2004).
8. C. Kanchanomai and Y. Mutoh, *J. Electron. Mater.* 33, 329 (2004).
9. C. Kanchanomai, Y. M., and Y. Mutoh, *J. Electron. Mater.* 31, 456 (2002).
10. C. Kanchanomai, Y. Miyashita, and Y. Mutoh, *J. Electron. Mater.* 31, 142 (2002).
11. Y. Kariya and M. Otsuka, *J. Electron. Mater.* 27, 1229 (1998).
12. H.L. John, B.S. Pang, T.H. Xiong, and Low, *Thin Solid Films* 462–463, 408 (2004).
13. H.L. John, B.S. Pang, T.H. Xiong, and Tow, *Int. J. Fatigue* 26, 865 (2004).
14. Y. Kanda and Y. Kariya, *J. Electron. Mater.* 39, 238 (2010).
15. Y. Kanda, Y. Kariya, and Y. Mochizuki, *Mater. Trans.* 49, 1524 (2008).
16. J. Liang, S. Downes, D. Shangguan, and S.M. Heinrich, *J. Electron. Mater.* 33, 1507 (2004).
17. ASTM Standards, ASTM E606, *Standard Practice for Strain-Controlled Fatigue Testing*, Vol. 03.01 (West Conshohocken, PA: The American Society for Testing and Materials, 1998).
18. C.K. Lin and C.M. Huang, *J. Electron. Mater.* 35, 292 (2006).
19. Y. Ding, C. Wang, and M. Li, *J. Electron. Mater.* 34, 1324 (2005).
20. T.-M.K. Korhonen, L.P. Lehman, M.A. Korhonen, and D.W. Henderson, *J. Electron. Mater.* 36, 173 (2007).
21. K.O. Lee, Yu Jin, T.S. Park, and S.B. Lee, *J. Electron. Mater.* 33, 249 (2004).
22. W.H. Kim and C. Laird, *Acta Metall.* 26, 777 (1978).
23. J.H.L. Pang, D.Y.R. Chong, and T.H. Tow, *IEEE Trans. Compon. Packag. Technol.* 24, 705 (2001).
24. X.Q. Shi, H.L.J. Pang, W. Zhou, and Z.P. Wang, *Int. J. Fatigue* 22, 217 (2000).
25. X.P. Zhang, C.B. Yu, S. Shrestha, and L. Dorn, *J. Mater. Sci. Mater. Electron.* 18, 665 (2007).
26. M. Amagai, *Microelectron. Reliab.* 39, 463 (1999).
27. C. Kanchanomai, Y. Miyashita, Y. Mutoh, and S.L. Mannan, *Mater. Sci. Eng. A* 345, 90 (2003).